

UNCLASSIFIED

SLL 80 570
Copy 1

AEROSPACE REPORT NO.
ATR-79(8408)-2

file: (A)

LASERS
AO, OL, S

Calibration of Piezoelectric Driven Mirrors for Laser Resonators

Prepared by
R. L. VARWIG, R. L. SANDSTROM (Consultant), and C. P. WANG
Aerophysics Laboratory

21 September 1979

DISTRIBUTION STATEMENT A
Approved for public release
Distribution Unlimited

Prepared for
VICE PRESIDENT AND GENERAL MANAGER
LABORATORY OPERATIONS



Laboratory Operations
THE AEROSPACE CORPORATION

PLEASE RETURN TO:

**BMD TECHNICAL INFORMATION CENTER
BALLISTIC MISSILE DEFENSE ORGANIZATION
7100 DEFENSE PENTAGON
WASHINGTON D.C. 20301-7100**

DTIC QUALITY INSPECTED

U4054

19980309 341

UNCLASSIFIED

Accession Number: 4054

Publication Date: Sep 21, 1979

Title: Calibration of Piezoelectric Driven Mirrors for Laser Resonators

Personal Author: Varwig, R.L.; Sandstrom, R.L.; Wang, C.P.

Corporate Author Or Publisher: Aerospace Corporation, El Segundo, CA 90245 Report Number: ATR-79(8408)-2

Report Prepared for: Space and Missile Systems Division, Air Force Systems Command, Los Angeles, CA 90045 Report Number Assigned by Contract Monitor: SLL 80 570

Comments on Document: Archive, RRI, DEW

Descriptors, Keywords: Calibration Piezoelectric Drive Mirror Laser Resonator Acoustooptics Modulator Heterodyne Frequency Modulate Conventional Interferometer

Pages: 19

Cataloged Date: Dec 09, 1992

Document Type: HC

Number of Copies In Library: 000001

Record ID: 25572

Source of Document: DEW

UNCLASSIFIED

Aerospace Report No.
ATR-79(8408)-2

CALIBRATION OF PIEZOELECTRIC
DRIVEN MIRRORS FOR LASER RESONATORS

Prepared by

R. L. Varwig, R. L. Sandstrom (Consultant), and C. P. Wang
Aerophysics Laboratory

21 September 1979

Laboratory Operations
THE AEROSPACE CORPORATION
El Segundo, California 90245

Prepared for

VICE PRESIDENT AND GENERAL MANAGER
LABORATORY OPERATIONS

UNCLASSIFIED

CALIBRATION OF PIEZOELECTRIC
DRIVEN MIRRORS FOR LASER RESONATORS

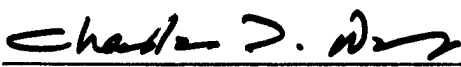
Prepared



R. L. Varwig



R. L. Sandstrom



C. P. Wang

Approved



H. Mirels, Head
Aerodynamics and Heat Transfer
Department



W. R. Warren, Jr., Director
Aerophysics Laboratory

ABSTRACT

A new technique for measuring small displacements of piezoelectric driven mirrors in which is employed an acousto-optic modulator and optical heterodyning has been applied to the calibration of piezoelectric driven mirror systems for laser resonator cavities. In this technique, a phase detector is used to measure the phase change when a mirror, driven by the piezoelectric translator, moves. Measurements obtained by means of this technique have been compared with measurements obtained with the traditional interferometer methods and have proven to be more precise. The increased precision was attributed to higher signal-to-noise ratios typically obtained with frequency-modulated, relative to amplitude-modulated, systems where intensity fluctuations exist in the system. The increased signal-to-noise ratio is advantageous when, as frequency increases, the output voltage from the driving power amplifier falls off. For a given amplifier, frequency response data of the piezoelectric driver-mirror combination can be determined at higher frequencies. In the case at hand, the frequency has been extended from 15 to 40 kHz.

ACKNOWLEDGMENTS

It is with pleasure that the authors recognize the contributions of Mr. Terry Felker, who provided technical support for the test program.

CONTENTS

ABSTRACT	v
ACKNOWLEDGMENTS	vi
I. INTRODUCTION	1
II. MEASUREMENTS	3
A. Acousto-Optic Modulator Phase Detector Method	3
B. Conventional Interferometer Method	7
III. RESULTS AND CONCLUSIONS	15
IV. SUMMARY	17
APPENDIX. CALCULATION OF PZT CALIBRATION	A-1

FIGURES

1.	Acousto-Optic Modulator Arranged to Measure Mirror Motions	4
2.	Phase Detector Calibration of PZT Units S/N-1 and -2 and Burleigh High-Frequency PZT Unit at 1 kHz	6
3.	Schematic Diagram for Measuring Displacement of Mirror with Zygo Interferometer when Driven by Piezoelectric Ceramic Normal to its Surface	8
4.	Fringe Pattern	9
5.	Typical Fringe Shift Pattern for Determining Calibration of PZT Unit S/N-2	10
6.	Frequency Response of 4 Folar PZT Units as Determined with Phase Detector	13
7.	Zygo Interferometer Calibration Measurements of S/N-1 and -2 and Burleigh High-Frequency PZT Units at 1 kHz	16

I. INTRODUCTION

Piezoelectric (PZT) ceramic components, either disks or cylinders, are used to drive the mirrors in laser resonator cavities to change the resonator length and, hence, the resonator frequency. Therefore, the calibration of the PZT unit, i. e., the change in length per unit drive voltage, must be known. The frequency response of the PZT unit and its electrical driver is also of importance in determining loop gain when the unit is used in a feedback control circuit for stabilizing the laser.

In this report, a new technique for measuring the small displacements required for PZT calibration is described in which an acousto-optic modulator and optical heterodyning are used. In this technique, zeroth- and first-order diffracted beams from the acousto-optic modulator serve as measuring and reference beams in a phase-detecting system used to measure a change in phase when a mirror driven by the PZT to be calibrated moves. The phase variation is obtained when the two beams are combined in a heterodyning technique. The resultant beat signal, carrying the phase modulation, is demodulated, and the signal is displayed on an oscilloscope.

Measurements obtained with this technique are compared with a traditional interferometer measurement. The advantages of each system are described.

II. MEASUREMENTS

A. ACOUSTO-OPTIC MODULATOR PHASE DETECTOR METHOD

The experimental arrangement for measuring small displacements with the acousto-optic modulator phase detector is shown in Fig. 1. An acoustic wave establishes a pattern of density variations in an acoustic medium, which then becomes a moving phase grating. An optical wave passing through the medium normal to the acoustic wave direction is split into N diffracted beams oriented according to $\sin \theta_N = N\lambda/\Lambda$. Here, λ is the optical wavelength, Λ is the acoustic wavelength, and N , an integer, is the order of diffraction. For a Flint glass acoustic medium, $\Lambda = 87.7 \mu\text{m}$ for a 40-MHz acoustic wave; $\lambda = 0.6328 \mu\text{m}$, so that $\theta_1 = 0.41$ deg, which agrees quite well with the measured value of 0.4 deg.

Light in the diffracted beams has vector components along the axis of acoustic propagation and, therefore, experiences a frequency shift as a result of the Doppler effect

$$\omega_N = \omega + N\Omega$$

where ω and Ω are the optical and acoustic frequencies, respectively. In the phase detector, as used here, the zeroth- and first-order diffracted beams are combined by a beam splitter-mirror combination so that they constructively interfere with each other. The photodetector, a 1P28 photomultiplier tube, by observing the signal, detects the beat-frequency signal between these two beams.

The PZT to be calibrated drives mirror normal to its surface. From geometrical considerations, the phase change in terms of wavelength and mirror displacement Δ is

$$m = \frac{2\Delta}{\lambda} \left[1 + 0 \left(\frac{\beta}{2} \right)^2 \right]$$

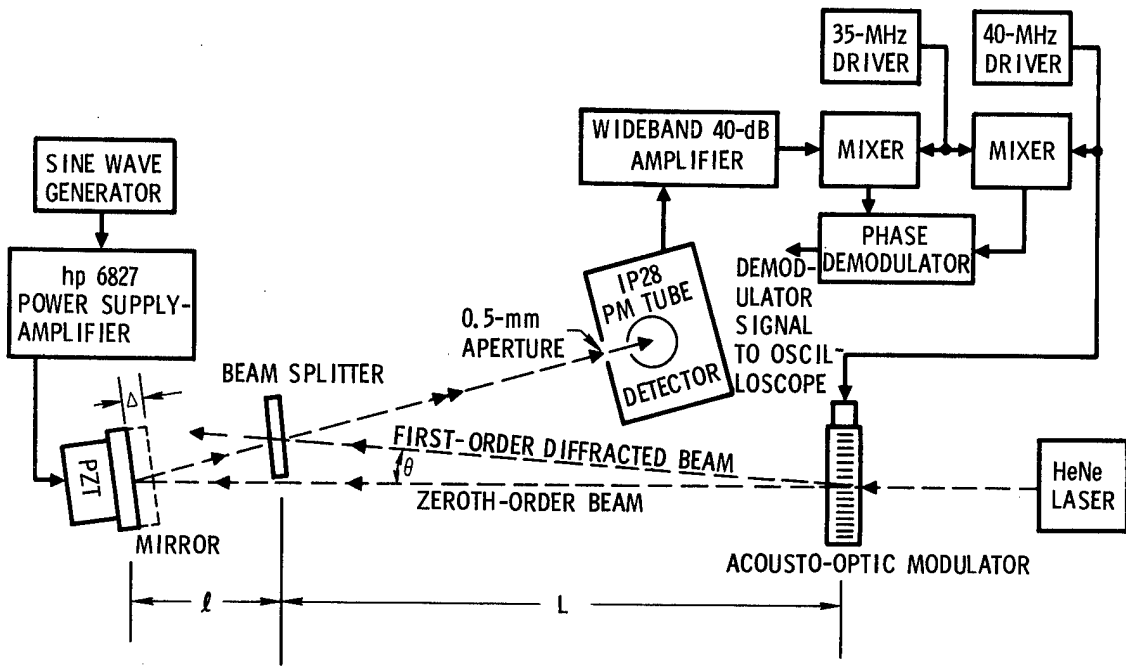


Fig. 1. Acousto-Optic Modulator Arranged to Measure Mirror Motions

where β is the angle of incidence of the light on the mirror. Since β is small (Fig. 1), the phase change as the mirror moves is $m = 2\Delta/\lambda$ or $2\pi(2\Delta/\lambda)$ rad or $(2\Delta/\lambda) 360$ deg.

The phase is determined by means of the phase demodulator in Fig. 1. This circuit mixes the carrier signal, the beat frequency Ω , containing the phase-varying modulation from the mirror perturbation, with a reference signal and provides the demodulated output (the difference frequencies) by low-pass filtering. The circuit is tuned to 5 MHz; therefore, a 35-MHz signal is beat with the 40-MHz carrier to provide a 5-MHz carrier. Similarly, the reference signal is obtained by beating the unmodulated 40-MHz driver signal with the 35-MHz signal. Sensitivity of the phase demodulator circuit is 200 deg/V, which was determined by use of a phase-shifting circuit that operated at 5 MHz and had as its output a 5-MHz signal with a shifted phase. The phase shift was set at 2π rad by comparing an input 5-MHz signal and a phase-shifted signal on an oscilloscope. Then, the phase-shifted signal was applied to the phase demodulator, and the output signal observed. The phase demodulator signal was 1.8 V for 2π or a 360-deg phase shift.

PZT calibration is determined by driving the mirror with an oscillating signal of known value V_D , the lower trace of Fig. 2. The phase variation is determined by the output of the phase demodulator V_S , the upper trace of Fig. 2. From these signal levels (in volts) plus the phase-demodulator calibration of 200 deg/V, the mirror calibration is

$$\text{Calib} = \left(\frac{200 \text{ deg}}{\text{V}} \right) \left(\frac{\lambda}{2} \right) \left(\frac{1}{360 \text{ deg}} \right) \frac{V_S}{V_D} = \frac{\lambda}{3.6} \left(\frac{V_S}{V_D} \right) \frac{\mu\text{m}}{\text{V}}$$

Numerical results are discussed in a later section.

Phase Detector Calibration of PZT Units S/N-1, 2 and Burleigh High Frequency PZT Unit at 1 kHz

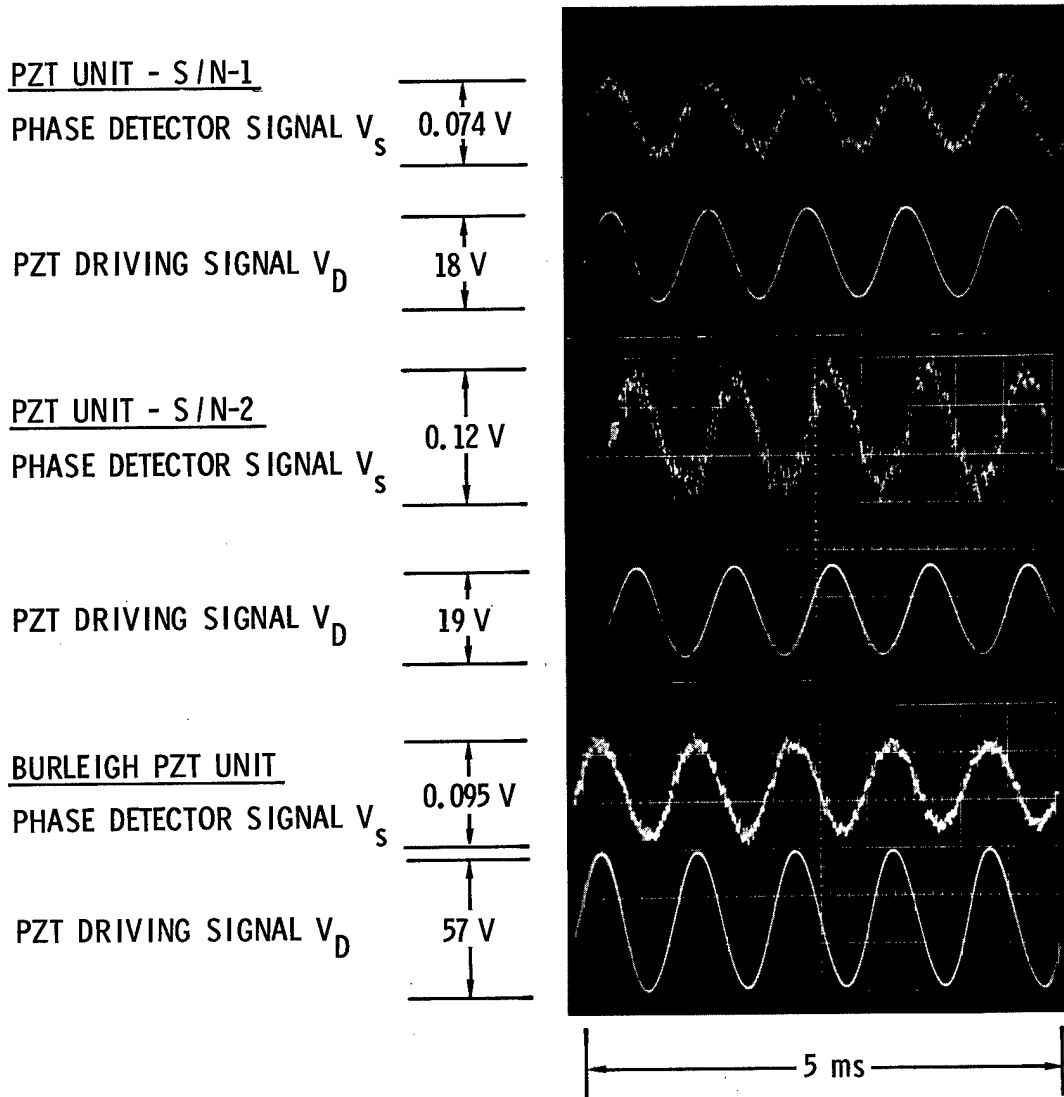


Fig. 2. Phase Detector Calibration of PZT Units S/N-1 and 2 and Burleigh High-Frequency PZT Unit at 1 kHz

B. CONVENTIONAL INTERFEROMETER METHOD

Traditional interferometer measurements were made for comparison by means of the arrangements shown in Fig. 3. Here, a Zygo interferometer (Zygo Corporation, Middlefield, Connecticut), which is a type of Fizeau interferometer, was used. A HeNe laser ($0.6328 \mu\text{m}$) is used as the light source, so that the coherence length is large. Straight fringes are formed by the wedge-shaped film between the reference mirror of the interferometer and mirror mounted on the PZT to be tested. These fringes are observed in the film plane of the interferometer, where a pinhole aperture and 1P28 photomultiplier tube are installed. When the mirror is driven normal to itself, the wedge thickness varies, causing the fringes to shift. By careful adjustment of the wedge angle, a single fringe can be obtained that covers the film plane (Fig. 4). Hence, the resolution of the fringe variation can be maximized. Fringe resolution is indicated in Fig. 4 by the relative size of the aperture and the fringe spacing. A typical fringe shift pattern obtained with this assembly is shown in Fig. 5. The lower trace of Fig. 5 is the driving voltage applied to the PZT-mirror unit and, therefore, represents the oscillatory motion of the mirror. The upper trace is the intensity variation as the fringe shown in Fig. 4 shifts across the detector aperture. Thus, starting at point A with the mirror moving in one direction, a bright fringe passes the aperture, point B. As the mirror continues in the same direction, the bright fringe shifts to dark, point C. At point D, the mirror motion is reversed. For a fringe shift from bright to dark, the length change is $(1/2)\lambda$, but since both incident and reflected paths must be included, this distance corresponds to a mirror motion of one-fourth wavelength. Thus, a direct calibration of the PZT-driven mirror unit is obtained, i.e., the mirror moves $\lambda/4 = 0.1582 \mu\text{m}$ for a signal change $V_B - V_C = 140 \text{ V}$, yielding a calibration of $1.13 \mu\text{m/kV}$. The capability for providing a direct calibration represents the chief advantage of the interferometer technique.

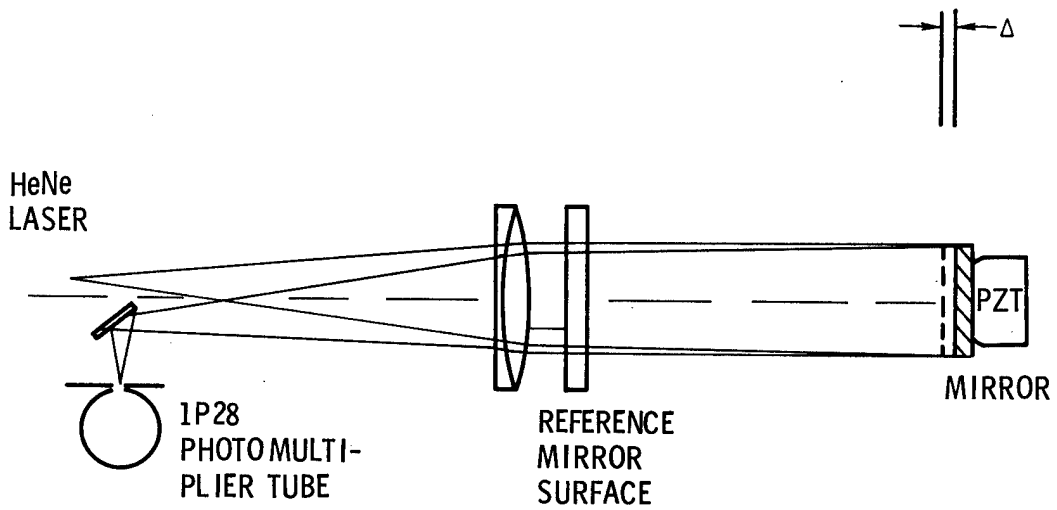


Fig. 3. Schematic Diagram for Measuring Displacement of Mirror with Zygo Interferometer when Driven by Piezoelectric Ceramic Normal to its Surface

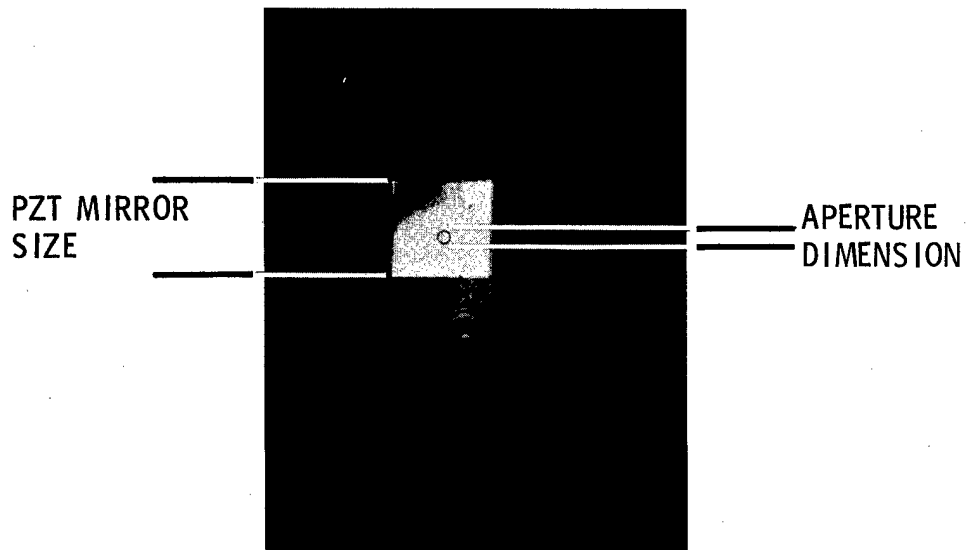


Fig. 4. Fringe Pattern (In this case, a single fringe, in the Zygo interferometer is shown with the photo detector aperture image.)

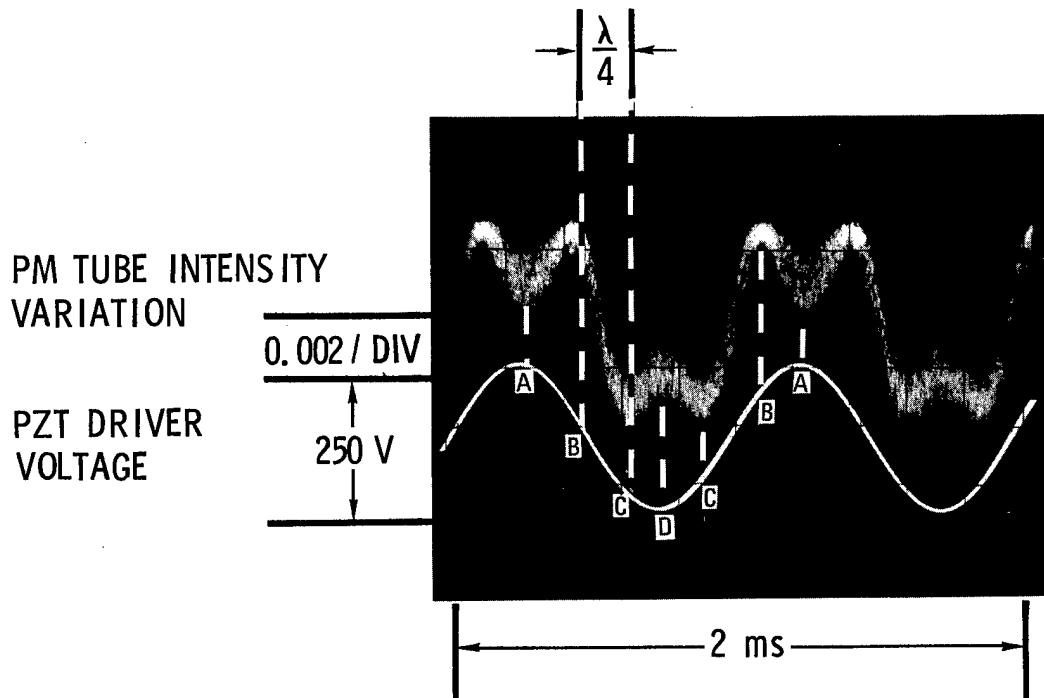


Fig. 5. Typical Fringe Shift Pattern for Determining Calibration of PZT Unit S/N-2. (A complete shift from center of bright fringe B to center of dark fringe C is observed, which corresponds to $(1/4)\lambda = 0.1582 \mu\text{m}$. $\Delta V = V_B - V_C$ for this shift is 140 so that calibration is $1.13 \mu\text{m/kV}$)

Values from the calibration measurement for four PZT units with mirrors from both the phase detector and the Zygo interferometer are given in Table 1, together with the calculated or estimated values determined from the physical properties of the PZT units. These predictions are described in the appendix.

The measured values for the calibration factor for the units Serial No. 1 (S/N-1) and Serial No. 2 (S/N-2), which are two-disk units made from 1.27-cm-diameter (0.5 in.) by 0.127-cm-thick (0.05 in) disks of a ceramic manufactured by Vernitron Corporation, Bedford, Ohio, and designated as PZT-5H, are different from each other by about a factor of two, which indicates that one of the two disks in the stack making up S/N-1 is disabled. Probably no contact has been established between one of the tabs on the unit and the silver plating deposited on each surface of the disk.

Frequency-response data for these PZT units are presented in Fig. 6. These data were obtained by plotting the ratio of the photomultiplier output signal to the driving voltage signal as a function of frequency. An hp 6827 bipolar power supply-amplifier serves as the driver amplifier for the laboratory-built S/N-1 and S/N-2 and the Burleigh high-frequency PZT units, whereas a Burleigh PZ-70 operational amplifier was used to drive the PZ-80 unit.

The Burleigh PZ-80, with its cylindrical construction and heavier mirror and retaining ring assembly, should have a lower resonant frequency relative to the disk-type PZT drivers, which is, in fact, observed. A resonant peak in the gain versus frequency curve occurs at about 4 kHz. The gain falls off rapidly beyond 4 kHz. Since the gain versus frequency curve is flat to 1 kHz, this unit should provide adequate response to that frequency. The other three units examined all appeared to remain flat to beyond 10 kHz. At between 15 and 30 kHz, the hp 6827 amplifier begins to fall off, which probably explains the bobble in the gain-frequency curves that appears to start at 15 kHz. There is a cutoff filter in the phase demodulator at 40 kHz. Hence, no measurements are obtained beyond this

point. It can be concluded that these three PZT units along with their mirrors and amplifier can be used quite satisfactorily to a frequency of 15 kHz.

Table 1. Calibration Factors Obtained for PZT Units

PZT Unit	Zygo Calibration, $\mu\text{m}/\text{V}$	Phase-Detector Calibration, $\mu\text{m}/\text{V}$	Value Computed from PZT Property, $\mu\text{m}/\text{V}$
Burleigh High Frequency	0.000394	0.000316	0.0003
Laboratory- Built S/N-1	0.000662	0.0012	0.0012
Laboratory- Built S/N-2	0.00151	0.00104	0.0012
Burleigh PZ-80	0.0049	0.00478	0.0043 0.0096

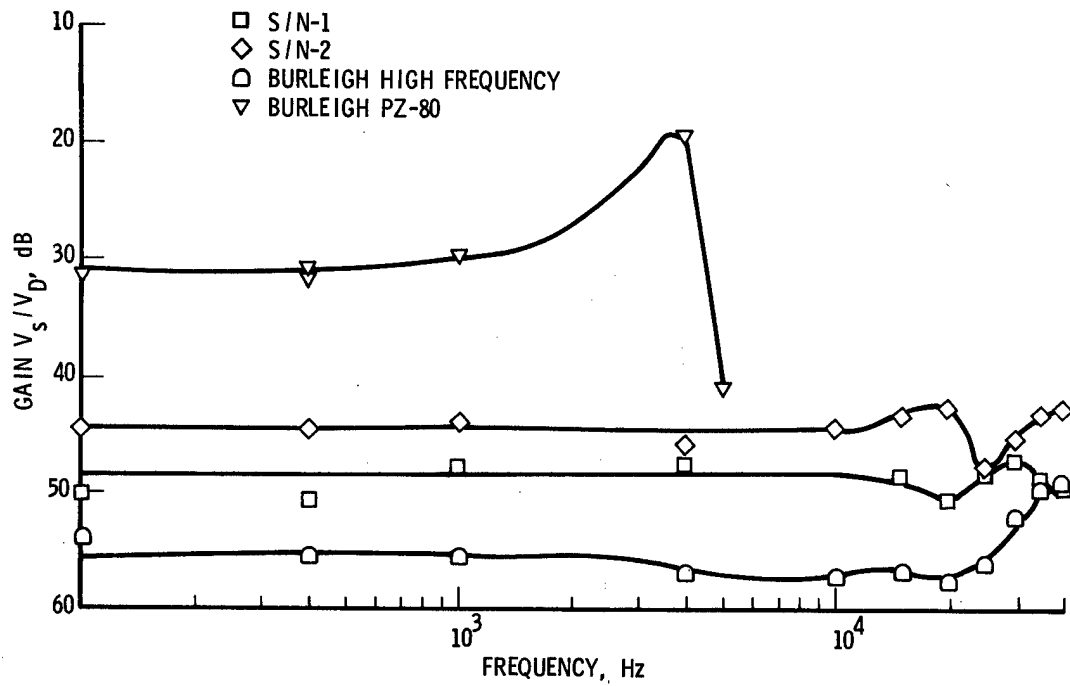


Fig. 6. Frequency Response of Four PZT Units as Determined with Phase Detector

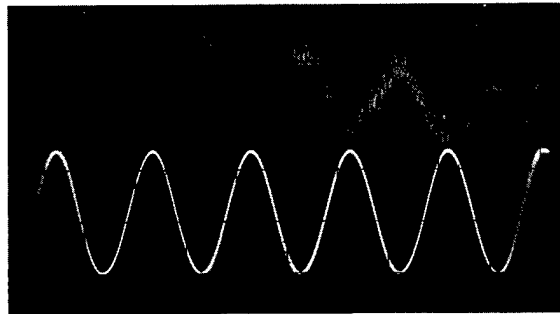
III. RESULTS AND CONCLUSIONS

Data for the calibration of three PZTs have been obtained with the acousto-optic modulator phase detector and, for comparison, the Zygo interferometer. Oscilloscope records of these data are shown in Fig. 2 for the phase detector and in Fig. 7 for the interferometer. The advantage of the phase detector over the interferometer is obvious. Its signal-to-noise ratio is 40 times greater than that of the interferometer when referenced to the PZT driving signal, because in phase modulation, half of the noise is rejected by clipping of the input signal. Thus, the effect of fringe drift and jiggle, which the interferometer observes is reduced in the phase detector. In addition, the advantage of phase modulation over amplitude modulation is wider bandwidth. Also, more complex side-band frequency structure contributes to higher signal-to-noise ratio in the phase detector.

One of the objectives of this study is to obtain frequency-response data of the PZT mirror mount. These data are obtained by observing the phase detector or interferometer signal while increasing the signal frequency driving the PZT. As with all amplifiers, as frequency increases, a point is reached where the amplifier output voltage falls off. Thus, the signal driving the PZT is decreased so that the PZT displacement is reduced. With decreased mirror displacement, signal size is reduced so that signal-to-noise ratio decreases. The output voltage driving PZT S/N-2, for example, drops to 20 V at a frequency of 40 kHz. The phase-detector output is easily observed at 40 kHz. However, for the interferometer, a 20-V oscillation signal on the PZT would produce a signal less than one-third the signal observed (top trace for PZT S/N-2, Fig. 7). Such a value would be indistinguishable from the noise on this signal. As a result, one is unable to obtain frequency-response data at frequencies close to 40 kHz with the interferometer technique. The practical limit is probably closer to 15 kHz.

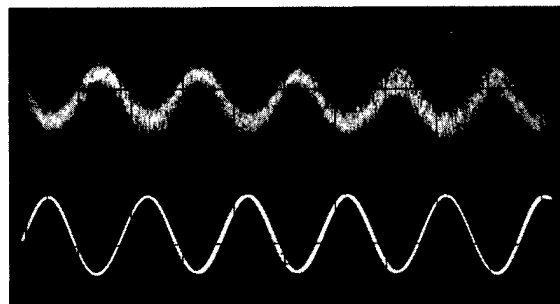
PZT UNIT - S/N-1
PHOTOMULTIPLIER
TUBE INTENSITY
VARIATION
PZT DRIVING SIGNAL

0.001 V
170 V



PZT UNIT - S/N-2
PHOTOMULTIPLIER
TUBE INTENSITY
VARIATION
PZT DRIVING SIGNAL

0.0016 V
75 V



BURLEIGH HIGH FREQUENCY
PZT UNIT
PHOTOMULTIPLIER
TUBE INTENSITY
VARIATION

0.0012 V
270 V

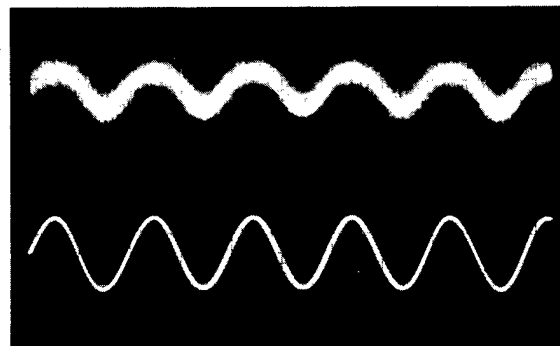


Fig. 7. Zygo Interferometer Calibration Measurements of S/N-1 and -2 and Burleigh High-Frequency PZT Units at 1 kHz. (Intensity variation results from fringe shift in interferometer.)

IV. SUMMARY

The phase detector devised by the Laboratory Operations, The Aerospace Corporation, has been applied to the problem of measuring small displacements for calibrating piezoelectric drivers for tuning laser cavities. The measurements were compared with those obtained from a traditional interferometer technique and found to be superior from the standpoint of signal-to-noise ratio. As a result of this superiority, frequency-response measurements of PZT units were pushed to higher levels with improved precision.

APPENDIX

CALCULATION OF PZ T CALIBRATION

For a thickness mode vibration of a PZT unit, the electrical field and displacement or strain are in the same direction (Fig. A-1). The change in thickness Δt is, therefore, given by $\Delta t = Nd_{33} V$, where N is the number of disks in the PZT stack and d_{33} is the piezoelectric constant in the thickness direction. For PZT-5H, $d_{33} = 593 \times 10^{12}$ m/V. V is the voltage across each disk. The disks are connected electrically in parallel for PZT units S/N-1 and 2. This relation yields

$$\begin{aligned}\Delta t &= 2(593) (10^{-5}) \mu\text{m}/V \\ &= 0.00119 \mu\text{m}/V\end{aligned}$$

for the PZ-80 unit, which is similar to a hollow cylinder in which the length changes for electric field applied normal to the cylinder walls (Fig. A-2). The change in length is determined according to

$$d_{31} = \frac{\Delta}{l} \frac{t}{V}$$

where d_{31} is the piezoelectric constant for length change normal to electric field direction, l is the cylinder length, and t is the cylinder wall thickness. From Vernitron Corporation data, d_{31} is between -123 and -274 10^{-12} m/V. The cylinder is 4.44 cm long, with a wall thickness of 0.127 cm. From these values, the displacement is

$$\Delta = 0.0043 \text{ to } 0.0096 \mu\text{m}/V$$

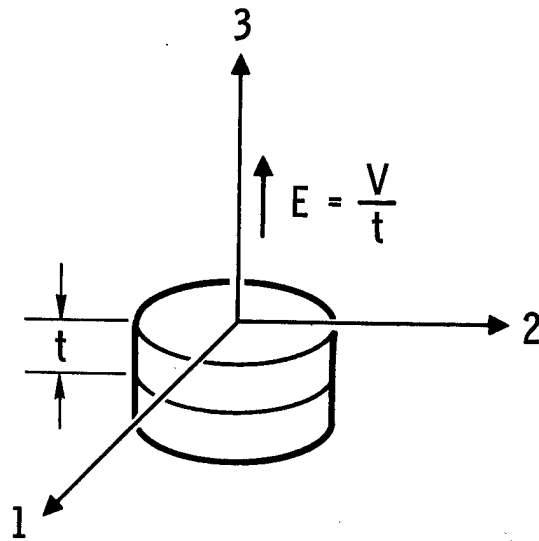


Fig A-1. Disk-Type PZT Element

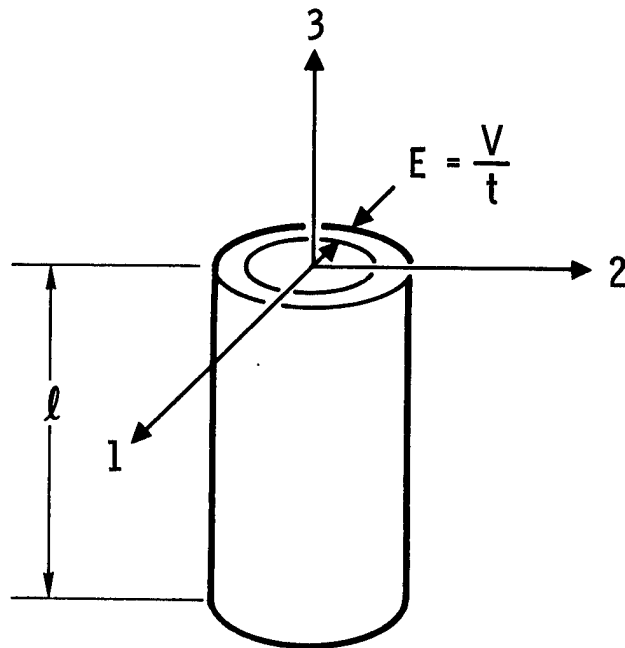


Fig. A-2. Cylindrical-Type PZT Element

DISTRIBUTION

Internal

P. J. Ackman
R. M. Allman
J. W. Berkovec
J. M. Bernard
M. Birnbaum
R. A. Chodzko
J. G. Coffey
N. Cohen
E. F. Cross
M. K. Dubas
D. A. Durran
J. W. Ellinwood
M. Epstein
T. L. Felker
R. R. Giedt
D. J. Griep
R. W. F. Gross

K. E. Hagen
D. T. Hodges, Jr.
R. Hofland
M. A. Kwok
A. C. Liang
S. B. Mason
H. Mirels
D. H. Ross
P. L. Smith
D. J. Spencer
E. B. Turner
R. L. Varwig
C. P. Wang
W. R. Warren, Jr.
M. T. Weiss
J. S. Whittier
R. L. Wilkins

External

SAMSO

Attn: Lt. Col. Lindemuth (DYXT)
Lt. J. C. Garcia (DYXT)
Lt. Col. H. Shelton (YNAD)
Mr. G. E. Aichinger (TM)
Maj. Kosalka (LVO)
Maj. Simondi (LVO)

AVCO-Everett Research Laboratory
2385 Revere Beach Parkway
Everett, MA 02149
Attn: Dr. G. W. Sutton
Dr. J. Daugherty
Dr. R. Limpaecher

AFWL

Kirkland AFB, NM 87117
Attn: Col. J. Rich (AR)
Lt. Col. A. D. Maio (AL)
Dr. P. Avizonis (AL)
Capt. B. Crane (ALC)
Dr. L. Wilson (ALC)
Lt. Col. D. Olson (ALC)
Mr. L. Rapagnani (ALC)

Bell Aerospace Textron
P.O. Box 1
Buffalo, NY 14240
Attn: Dr. W. Solomon/Mail Zone B-49
Dr. J. W. Raymond/
Mail Zone B-49
Dr. R. J. Driscoll/
Mail Zone B-49

DARPA
1400 Wilson Blvd.
Arlington, VA 22209
Attn: Dr. H. A. Pike
Dr. J. Mangano
Dr. R. Sepucha

Undersecretary of the Air Force
The Pentagon
Washington, DC 20330
Attn: Dr. Hans Mark

AFRPL (LKCG)
Edwards AFB, CA 93523
Attn: B. R. Bornhorst

Los Alamos Scientific Laboratory
P. O. Box 1663
Los Alamos, NM 87544
Attn: Dr. K. Boyer
Dr. E. Brock
Dr. G. Emanuel/Sta AP-DO 563
Dr. R. Jensen
Dr. G. Kyrala/P-1-455
Dr. E. O'Hair
Dr. J. Parker/Sta 548
Dr. S. Rockwood

Deputy Chief of Staff for Research,
Development and Acquisition
Dept. of the Army, Headquarters
The Pentagon
Washington, DC 20310
Attn: Lt. Col. B. J. Pellegrini/3B482

US Army Missile Research and
Development Command
Redstone Arsenal, AL 35809
Attn: DRDMI-HS (Mr. J. M. Walters)
DRSMI-RK (Dr. W. Wharton)
DRSMI-RH (Dr. T. A. Barr, Jr.,
Dr. D. Howgate)

Deputy Asst. Secretary of the Navy
(Research and Advanced Technology)
Pentagon, Rm 4 D 745
Washington, DC 20350
Attn: Dr. T. A. Jacobs
Dr. R. Hoglund

California Institute of Technology
Pasadena, CA 91109
Attn: Prof. A. Kuppermann
Prof. H. Liepmann
Prof. A. Roshko

CALSPAN Corporation
P. O. Box 235
Buffalo, NY 14221
Attn: Dr. J. Daiber
Dr. C. E. Treanor

Columbia University
Dept. of Chemistry
New York, NY 10027
Attn: Dr. R. Zare

Michigan State University
Dept. of Mechanical Engineering
E. Lansing, MI 48824
Attn: Dr. R. Kerber

Cornell University
Ithaca, NY 14853
Attn: Dr. T. A. Cool, Applied Physics
Dr. S. H. Bauer, Chemistry

General Electric Company
U7211 VFSTC
P. O. Box 8555
Philadelphia, PA 19101
Attn: R. Geiger
J. Gilstein

Hughes Research Laboratory
3011 Malibu Canyon Road
Malibu, CA 90265
Attn: Dr. A. Chester

Hughes Aircraft Company
Centinella and Teale Street
Culver City, CA 90230
Attn: Dr. E. R. Peressini
Dr. M. Mann
Dr. S. N. Suchard

Naval Research Laboratory
4550 Overlook Ave., S. W.
Washington, DC 20375
Attn: Dr. W. S. Watt/Code 5540
Dr. J. M. MacCallum/
Code 5503 EOTP
Dr. S. K. Searles/Code 5540
Dr. K. Whitney/Code 5565

Naval Sea Systems Command
Washington, DC 20362
Attn: Dr. D. Kinkleman PMS-405-20
Dr. L. Stoessell PMS-405-30
Dr. J. A. Stregack PMS-405-23
Capt. A. Skolnick PMS-405

Naval Surface Weapons Center
White Oak Laboratory
Silver Springs, MD 20910
Attn: Code WA-13/Bldg 405/Rm 219

Commander
Naval Weapons Center
China Lake, CA 93555
Attn: E. Lunstrom/Code 4011
H. E. Bennett

NASA Lewis Research Center
21000 Brook Park Road
Cleveland, OH 44135
Attn: S. Cohen/M.S. 500-209

NASA Ames Research Center
Moffett Field, CA 94035
Attn: Dr. C. F. Hansen

Defense Documentation Center
Cameron Station
Alexandria, VA 22314

RADC/ETSL
Hanscom Air Force Base, MA 01731
Attn: Dr. H. Schlossberg

Lockheed Missiles and Space Company
P.O. Box 1103, West Station
Huntsville, AL 35807
Attn: Dr. S. C. Kurzius

Lockheed Missiles and Space Company
4800 Bradford Blvd.
Huntsville, AL 35812
Attn: J. W. Benefield

Martin-Marietta
Denver, CO 80202
Attn: Dr. J. Bunting

Massachusetts Institute of Technology
Cambridge, MA 02139
Attn: Dr. A. Javan
Department of Physics
Dr. J. Steinfeld
Department of Chemistry

Mathematical Sciences Northwest, Inc.
P.O. Box 1887
Bellevue, WA 98009
Attn: Dr. S. Byron
Prof. A. Hertzberg
P. Rose
Dr. R. Center

McDonnell Douglas Corporation
5301 Bolsa Ave.
Huntington Beach, CA 92647
Attn: Dr. R. Lee/Bldg. 28, Rm 250
Dr. W. A. Gaubatz

McDonnell Research Laboratory
McDonnell Douglas Corporation
St. Louis, MO 63166
Attn: Dr. D. P. Ames
Dr. R. Haakinen
Dr. K. Kelly

Northrop Corporation
Research and Technology Center
1 Research Park
Palos Verdes Peninsula, CA 90274
Attn: Dr. M. L. Bhaumik

AFSC (DLS)
Andrews AFB
Washington, DC 20334

AFML (NA)
Wright-Patterson AFB, OH 45433

Air University Library
Maxwell AFB, AL 36112

Air Force Office of Scientific
Research
Bolling AFB, DC 20332
Attn: Directorate of Aerospace
Sciences (NA)
Directorate of Physics (NP)
Capt. Russell Armstrong

FJSRL (Tech Library)
USAF Academy, CO 80840

Scientific and Technical Info.
Facility (UNC)
P.O. Box 33
College Park, MD 20740 (A-Only)
Attn: NASA Representative

RADC (XP)
Griffiss AFB, NY 13442

Electric Power Research Institute
P.O. Box 10412
Palo Alto, CA 94303
Attn: Dr. W. Gough
Dr. N. Amhert

Department of Energy
Washington, DC 20545
Attn: Division of Laser Fusion
Dr. C. M. Stickley, Director
Dr. J. Weiss

Perkin-Elmer Corporation
Norwalk, CN 06856
Attn: M. L. Skolnick
Electro-Optical Division

Physics International Company
2700 Merced Street
San Leandro, CA 94577
Attn: Dr. B. Bernstein

Pratt and Whitney Aircraft Corporation
P.O. Box 2691 (B47 Mail Sta.)
West Palm Beach, FL 33402
Attn: Dr. G. H. McLafferty
Mr. R. Oglukian

Princeton University
Dept. of Aerospace and Mech. Science
Princeton, NJ 08540
Attn: Prof. S. Bogdonoff

Science Center
Rockwell International
1049 Camino Dos Rios
Thousand Oaks, CA 91360
Attn: Dr. A. T. Pritt, Jr.

BDM Corporation
2600 Yale Blvd, SE
Albuquerque, NM 87106
Attn: Dr. Robert D. Rose

Purdue University
School of Mechanical Engineering
Chaffee Hall
Lafayette, IN 47907
Attn: Prof. J. G. Skifstad

Rockwell International Corporation
Rocketdyne Division
Canoga Park, CA 91304
Attn: Dr. S. V. Gunn
Dr. A. Axworthy
Dr. E. Curtis
Dr. L. Zajac
Dr. T. T. Yang, BA32

Nuclear Research & Application
Advanced Isotope Separation
Technology
Washington, DC 20545
Attn: Dr. Kent Hancock
Mail Station H407

Lawrence Livermore Laboratory
P.O. Box 808
Livermore, CA 94550
Attn: Dr. J. Emmett
Dr. A. Karo

Arnold Engineering Development
Center
Arnold Air Force Station, TN 37389
Attn: L. R. Case (XOOE)

ODUS DRE (R&AT)
Rm 3E114 The Pentagon
Washington, DC 20301
Attn: Dr. G. P. Millburn
Dr. R. Airey

Deputy Undersecretary of Defense
(Strategic and Space Systems)
Rm 3E130 The Pentagon
Washington, DC 20301
Attn: Dr. S. Zeiberg

Deputy Undersecretary of Defense
(Tactical Warfare Programs)
Rm 3E1044 The Pentagon
Washington, DC 20301
Attn: Mr. R. A. Moore

University of Southern California
Department of Chemistry
Los Angeles, CA 90007
Attn: Prof. S. W. Benson
Prof. C. Wittig
Dept. of Electrical
Engineering

Science Applications, Inc.
6600 Powersferry Rd - Suite 220
Atlanta, GA 30339
Attn: Document Control

Science Applications, Inc.
2361 Jefferson Davis Highway
Arlington, VA 22202
Attn: Dr. Walter R. Sooy

TRW Systems Group
One Space Park
Redondo Beach, CA 90278
Attn: Dr. J. Miller 01/1080
Dr. D. Bullock
Dr. J. Stansel
Dr. C. W. Clendening, Jr.
R1/1016
Dr. P. Clark
Dr. R. Aprahamian

United Technologies Research
Laboratory
400 Main Street
East Hartford, CT 06108
Attn: Dr. J. Hinchin
Dr. A. Angelbeck
Dr. D. Seery
Dr. C. Ultee

University of Maryland
College Park, MD 20740
Attn: Dr. J. D. Anderson, Jr.
Head, Dept. of Aerospace
Engineering
College of Engineering

Wright State University
Dayton, OH 45431
Attn: Dr. T. O. Tiernan
Dr. G. D. Sides
Department of Chemistry

University of California, San Diego
Department of AMES
La Jolla, CA 92703
Attn: Prof. S. S. Penner
Prof. S. C. Lin

The Boeing Aerospace Company
Mail Stop 88-46
Seattle, WA 98124
Attn: Dr. J. D. McClure

IRIA Center
ERIM
P.O. Box 8618
Ann Arbor, MI 48107

W. J. Schafer Associates, Inc.
901 N. Ft. Myer Drive, Suite 803
Arlington, VA 22209
Attn: Dr. E. T. Gerry
Dr. W. Evers

W. J. Schafer Associates, Inc.
10 Lakeside Office Park
Wakefield, Mass. 01880
Attn: Dr. J. Reilly

Physical Sciences, Inc.
30 Commerce Way
Woburn, MA 01801
Attn: Dr. R. L. Taylor

The Department of Electrical
Engineering
University of Minnesota
123 Church Street, SE
Minneapolis, MN 55455
Attn: Professor Robert J. Collins

Center for Laser Studies
University of Southern California
Los Angeles, CA 90007
Attn: Professor Michael Bass